

From superfluid ^3He to altermagnets

T. Jungwirth,^{1,2} R. M. Fernandes,^{3,4} E. Fradkin,^{3,4} A. H. MacDonald,⁵ J. Sinova,⁶ and L. Šmejkal^{7,8,1}

¹*Institute of Physics, Czech Academy of Sciences, Cukrovarnická 10, 162 00, Praha 6, Czech Republic*

²*School of Physics and Astronomy, University of Nottingham, NG7 2RD, Nottingham, United Kingdom*

³*Department of Physics, University of Illinois Urbana-Champaign, Urbana, IL 61801, USA*

⁴*Anthony J. Leggett Institute for Condensed Matter Theory, University of Illinois at Urbana-Champaign, IL 61801, USA*

⁵*Department of Physics, The University of Texas at Austin, Austin, TX 78712, USA*

⁶*Institut für Physik, Johannes Gutenberg Universität Mainz, D-55099 Mainz, Germany*

⁷*Max Planck Institute for the Physics of Complex Systems, Nöthnitzer Str. 38, 01187 Dresden, Germany*

⁸*Max Planck Institute for Chemical Physics of Solids, Nöthnitzer Str. 40, 01187, Dresden, Germany*

(Dated: November 4, 2024)

The Pauli exclusion principle combined with interactions between fermions is a unifying basic mechanism that can give rise to quantum phases with spin order in diverse physical systems. Transition-metal ferromagnets, with isotropic ordering respecting crystallographic rotation symmetries and with a net magnetization, are a relatively common manifestation of this mechanism, leading to numerous practical applications, e.g., in spintronic information technologies. In contrast, superfluid ^3He has been a unique and fragile manifestation, in which the spin-ordered phase is anisotropic, breaking the real-space rotation symmetries, and has zero net magnetization. The recently discovered altermagnets share the spin-ordered anisotropic zero-magnetization nature of superfluid ^3He . Yet, altermagnets appear to be even more abundant than ferromagnets, can be robust, and are projected to offer superior scalability for spintronics compared to ferromagnets. Our Perspective revisits the decades of research of the spin-ordered anisotropic zero-magnetization phases including, besides superfluid ^3He , also theoretically conceived counterparts in nematic electronic liquid-crystal phases. While all sharing the same extraordinary character of symmetry breaking, we highlight the distinctions in microscopic physics which set altermagnets apart and enable their robust and abundant material realizations.

In his Nobel lecture¹, Anthony Leggett cautioned that "superfluid ^3He may well be the most practically useless system ever discovered", but also praised it as "probably the most sophisticated physical system of which we can claim a quantitative understanding". To frame the scope of our Perspective on altermagnets, let us begin in the following introductory paragraphs with briefly expanding on the first and second part of this quote.

Starting from the first part, it referred primarily to the fragile nature of the low-temperature superfluid phases of ^3He . The A-phase, which will serve as the central reference point in our discussion of altermagnets in this Perspective, is stabilized only within a narrow window of low temperatures around 2 mK and of high pressures around 30 bar. Coming to the second part of the quote, let us recall that the strongly repulsive interaction at short distances and attractive interaction at longer distances between the neutral spin-1/2 ^3He atoms favor an exotic Cooper paring with a non-zero relative angular momentum l . Moreover, the antisymmetric p-wave ($l = 1$) orbital part, together with the Pauli exclusion principle, implies a symmetric spin-triplet ($S = 1$) part of the pairing function. In the A-phase of superfluid ^3He , the Cooper pairs are a linear combination of ($l_z = 1, S_z = \pm 1$) states¹. This results in a spin-ordered superfluid condensate of the Cooper pairs which spontaneously breaks the continuous rotation symmetry of the spin space but has a zero net magnetization. Moreover, the phase is anisotropic, i.e., it also spontaneously breaks the continuous real-space rotation symmetry (Fig. 1).

Let us now compare this to ferromagnetism. In

analogy to superfluid ^3He , the spin-ordering in ferromagnets arises from the interactions in the Fermi fluid and the Pauli exclusion principle. The two again favor a symmetric spin part of, this time, a many-body wavefunction of charged spin-1/2 electrons, interacting via the repulsive Coulomb potential. This ferromagnetic-exchange mechanism of spin ordering is characterized by the broken spin-space rotation symmetry, like in superfluid ^3He . However, unlike superfluid ^3He , ferromagnets are isotropic in the sense that they preserve the discrete point-group rotation symmetries of the underlying crystal lattice.

We emphasize that in the above symmetry comparison between superfluid ^3He and ferromagnets, and throughout this entire Perspective, we omit the typically weak perturbative effects of the dipolar or relativistic spin-orbit coupling which lower the symmetry in the coupled spin and real space already at the level of the Hamiltonian of the system. Our focus is on the symmetry lowering by the ordered ground state in the limit of zero spin-orbit coupling which is, correspondingly, described by symmetry groups comprising pairs of generally distinct transformations in the spin space and in the real space. In analogy to the basic symmetry classification of the superfluid and superconducting phases^{2,3}, this approach has been also introduced in the recent classification of magnetic phases which has led to the delineation of altermagnets^{4,5}. (Relativistic spin-orbit coupling effects in altermagnets are reviewed in Refs. 6 and 7.)

Coming back to the comparison between superfluid

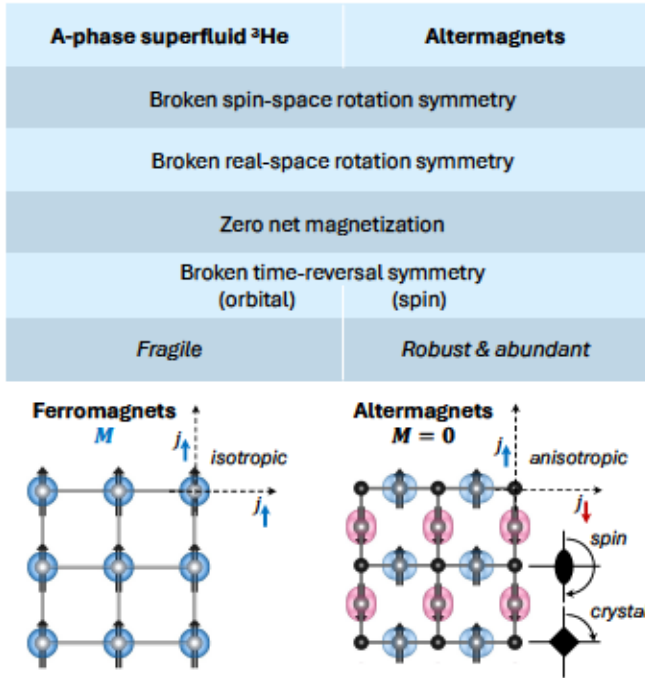


FIG. 1. A-phase superfluid ^3He , ferromagnets and altermagnets. Top panel: Analogous broken symmetries and zero net magnetization of the fragile A-phase of superfluid ^3He and the robust and abundant altermagnets. Bottom left panel: Isotropic ordering in a ferromagnet with a net magnetization (M) illustrated on a model square lattice. Spin-polarized currents ($j_{\uparrow(\downarrow)}$) respect the four-fold rotation symmetry of the crystal lattice (spin-orbit coupling is neglected). Bottom right: anisotropic ordering in an altermagnet with no net magnetization illustrated on a model square (Lieb) lattice. The spin arrangement on the crystal lattice has no symmetry combining a two-fold spin-space rotation with a real-space crystal translation or inversion. Simultaneously, it has a symmetry combining the two-fold spin-space rotation with a real-space crystal rotation (four-fold in the depicted model lattice). Spin-polarized currents break the four-fold rotation symmetry of the crystal lattice, with the polarization of the spin current flipping sign between the two orthogonal directions of the current flow.

^3He and ferromagnets, another distinction is that ferromagnets are characterized by a net magnetization. Besides the robustness and relative abundance of ferromagnets, the net magnetization underpins their practical utility. Here spintronic devices are among the recent highlights as they start to replace semiconductors in the technology of embedded non-volatile memories for advance-node processor chips^{8–10}. Their functionality is based on the spin-polarization of electrical currents, which is directly generated by the net magnetization (Fig. 1). Simultaneously, however, the net magnetization sets physical limits on the spatial, temporal and energy scalability of the ferromagnetic spintronic technology⁵.

Removing these limits was the practical incentive to search for magnets combining the spin-polarized currents with the absence of the net magnetization. This has

materialized in the recent discovery of altermagnets^{4,5} (Fig. 1). Expressed in a concise way, altermagnets can realize this extraordinary combination by featuring an alternating-sign spin polarization at neighboring sites with an alternating orientation of anisotropic local crystal environment (Fig. 1). Besides the resulting zero net magnetization, altermagnets share the exotic spin-ordered anisotropic nature of the A-phase of superfluid ^3He , and are also quantitatively understood¹¹.

We conclude these opening remarks by pointing out that counterparts of the spin-ordered anisotropic A-phase of superfluid ^3He have been theoretically discussed since more than thirty years ago in spin-ordered nematic electronic liquid-crystals^{12–16}. Their realization requires an intricate form of the interacting Fermi fluid to, among other limitations, outweigh the common isotropic ferromagnetic phase^{12,16}. This led to an expectation of a subtle and rare nature^{12,17} of these spin-ordered electronic nematics. Experimentally, they have remained elusive.

In contrast, altermagnets are predicted to be even more abundant than ferromagnets^{4,5}. They can range from insulators to superconductors^{4,5,18,19}, and spectroscopic measurements have already confirmed altermagnetism in semiconducting and metallic candidates with magnetic ordering above room temperature^{11,20–27}. What sets altermagnets apart is that they are stabilized by an interplay of the electronic exchange interaction and the ionic single-particle potential of the crystal-lattice with a suitable symmetry. As such, altermagnetism can emerge in materials covering a broad range of interaction strengths, from weakly-interacting metals to strongly-interacting Mott insulators^{4,5,7,28}.

In Sec. A we begin with an overview of phases without the spin ordering in a two-parameter space of interaction strength and conduction type, to see where anisotropic ordered phases breaking the real-space rotation symmetry fit in. They will serve as a background reference for the follow-up Sec. B discussing the spin-ordered anisotropic phases. The section starts with highlighting the unique position of superfluid ^3He , and with introducing the theoretically conceived counterpart phases of spin-ordered nematic electronic liquid-crystals. They will set the stage for the discussion of how the fragility or elusiveness of these phases has been sidestepped in the spin and crystal-symmetry based method for identifying altermagnets. In Sec. C, we comment on how this method can lead to the prediction of other robust variants of the spin-ordered anisotropic zero-magnetization phases beyond altermagnets. Sec. D summarizes our Perspective.

We note that this Perspective is not intended to give an overview of the more than four hundred studies that have been reported over the past two years since the initial theoretical delineation of the altermagnetic phase⁴. For this we refer to recent review articles covering several of the emerging theoretical and experimental research fronts of altermagnetism^{5–7,29}.

A. Anisotropic phases without spin ordering

Painted with a broad brush, we can make the following (non-exhaustive) classification of phases without spin ordering by the conduction type and interaction strength, as shown in Fig. 2. Starting from the bottom-left of the diagram, we have band insulators whose physics is described by an effective single-particle band picture featuring an energy gap separating completely filled bands from empty bands. The band-insulating phases are produced by quantum-interference effects of electrons in the periodic potential of the crystal lattice.

Metallic phases feature a Fermi surface separating the occupied and empty electronic states. Landau's Fermi liquid theory^{30,31} provides an elegant explanation why, in many metals, excited states near the Fermi surface can be represented by weakly interacting fermion quasiparticles. This is because the scattering phase-space for the excited states near the Fermi surface is drastically limited by the Pauli exclusion principle. The interacting and non-interacting Fermi surfaces thus coincide, and the quasiparticles' lifetime becomes infinite when approaching the Fermi surface. Normal metals falling into this weak-interaction Fermi-liquid regime are depicted in the middle-left part of the diagram in Fig. 2.

At sufficiently low temperatures, an arbitrarily weak attractive interaction (e.g. mediated by phonons) between the quasiparticles near the Fermi surface leads to the formation of Cooper pairs of opposite-spin and opposite-momentum quasiparticles, corresponding to a spin-singlet ($S = 0$) s-wave ($l = 0$) pairing function. The Fermi surface gives way to a fermionic excitation gap, and the Cooper pairs condense into the conventional BCS superconducting state³², which we correspondingly placed in the top-left part of Fig. 2.

All the effectively weakly-interacting phases mentioned so far have no spin order and are isotropic. Their momentum-dependent electronic structure, i.e., the valence-band energy iso-surfaces in the band-insulators, the Fermi surface in the normal metals, or the pairing (gap) function in the s-wave superconductors preserve the spin-space rotation symmetry and the real-space point-group symmetries of the underlying crystal lattice.

We now move to the unconventional superconductivity^{2,3} in the strongly-interacting part of the diagram in Fig. 2. Because of strong short-range repulsive interactions, electrons in the Cooper pairs favor anisotropic pairing with $l > 0$, similar to the case of ^3He . This breaks (some) rotation symmetries of the crystallographic point group of the underlying lattice. Unconventional d-wave ($l = 2$) cuprate superconductors belong to this class. The symmetric orbital part of the pairing function dictates, by the Pauli exclusion principle, an antisymmetric spin-singlet ($S = 0$) part of the pairing function. This implies that the phase is not spin-ordered, preserving the rotation symmetry of the spin-space.

The remaining forms of ordering highlighted in Fig. 2

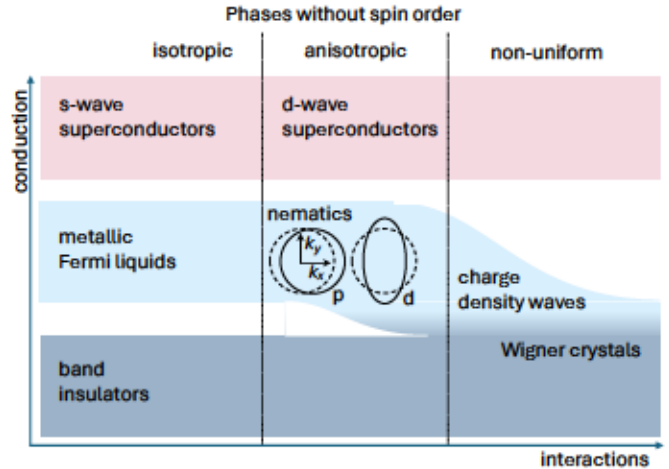


FIG. 2. **Phases without spin ordering.** Illustrative phases without spin ordering depicted in a conduction-type vs. interaction-strength diagram. Band insulators and metals (metallic Fermi liquids) are normal phases while the rest are ordered phases. Inset shows model Fermi surfaces of $l = 1$ (p-wave) and $l = 2$ (d-wave) nematic electronic liquid-crystal phases (solid lines), corresponding to shifted and anisotropically-distorted, resp., normal-phase Fermi surfaces (dashed lines). As explained in the main text, we use the term nematics in the generalized sense including all $l > 0$ even and odd-parity phases.

are non-superconducting. When the interaction energy dominates the kinetic energy at sufficiently low electronic densities, the electrons localize in a Wigner crystal. Apart from becoming insulating, the ordered phase is characterized by a non-uniformity, i.e., by a spontaneous breaking of the translation symmetry of the normal phase. Charge-density waves, stripe states or electronic smectic liquid crystals are other examples of correlated non-uniform ordered phases¹⁵. They can be insulating or metallic.

Finally, we arrive at the central part of the diagram in Fig. 2 corresponding to an intricate metallic intermediate-interaction regime of nematic electronic liquid crystals. Coming from the right, they can be viewed as melted smectic electronic liquid crystals^{15,33–36}, recovering the translation symmetry of the Fermi liquid, while retaining an anisotropic character¹⁵. Coming from the left, they can be described as Pomeranchuk Fermi-liquid instabilities in the $l > 0$ charge channel, characterized by anisotropic distortions of the Fermi surface (Fig. 2)^{15,37,38}. Simultaneously, the electronic nematics in Fig. 2 preserve the uniformity (translation symmetry) of the Fermi liquid, as well as the spin-space rotation symmetry. Note that in this article we use the term nematic electronic liquid-crystal phases in a generalized sense to underline the spontaneous breaking of the real-space rotation symmetry not only in the even-parity $l = 2$ case, which has been studied recently in various quantum materials, but in all even and odd-parity $l > 0$ phases^{14,17}.

We will elaborate on the framework of the Pomeranchuk Fermi-liquid instabilities in more depth in the next section where we move to the discussion of the spin-ordered anisotropic phases^{12,14,16,17,39–42}. Here we conclude the overview of the anisotropic phases without spin ordering by pointing out that the $l = 1$ Pomeranchuk instability has been a matter of an on-going discussion throughout the past hundred years. In Fig. 2, the instability is depicted as a Fermi-surface distortion in the form of a parity-breaking shift. From 1920's till 1940's, considered among others by Bloch, Landau or Born^{43–46}, such a Fermi-surface distortion, giving rise to a spontaneous equilibrium current, recurrently appeared as an attempt to explain conventional superconductivity. The theory failed as it violated the first theorem on superconductivity, formulated in the meantime by Bloch himself, showing that the minimum energy state bears no current⁴⁵. With the other unsuccessful theories at the time, it led Bloch to his "second theorem" stating that every theory of superconductivity could be disproved⁴⁵. While the conventional superconductivity was eventually explained by the Cooper-pairing mechanism³², whether or not the $l = 1$ Pomeranchuk instability is physically possible has remained a matter of theoretical research till today^{40–42}. Experimentally, it has remained elusive.

The $l = 2$ Pomeranchuk instability has a form of an even-parity anisotropic Fermi-surface distortion^{15,37,38} (Fig. 2). No principle constraint has been identified for this Pomeranchuk instability (or other $l > 2$ instabilities)⁴¹. The studied physical realizations include semiconducting 2D electron systems at high magnetic fields in the vicinity of correlated fractional quantum-Hall states, correlated ruthenates at high magnetic fields in the vicinity of a metamagnetic transition, as well as unconventional superconductors such as cuprates and iron pnictides^{15,38,47–52}.

B. Spin-ordered anisotropic phases and altermagnets

We now move to the discussion of spin-ordered anisotropic phases, i.e., phases that spontaneously break the spin-space rotation symmetry^{1,4,53}. Starting from the top of the diagram in Fig. 3, the well-established representative is superfluid ^3He . Already since late 1950's, more than a decade before the experimental discovery, theorists were considering extensions of the BCS theory to the case of charge-neutral spin-1/2 ^3He atoms, whose longer-range attractive interaction is complemented by a strong short-range repulsion¹. While this led to the prediction of Cooper pairing with non-zero angular momentum, the expectation was that ^3He would remain isotropic even in the superfluid phase. Specifically, for the spin-triplet p-wave pairing ($S = l = 1$), which was later confirmed experimentally, the lowest energy superfluid state originally predicted by the microscopic theory was formed by a condensation

of Cooper pairs given by a linear combination containing all three l_z values, $(l_z = -1, S_z = 1) + (l_z = 1, S_z = -1) + (l_z = 0, S_z = 0)$. While this state breaks rotational symmetry individually in the spin space and the orbital space, the total angular momentum $\mathbf{l} + \mathbf{S} = 0$ renders this so-called B-phase of superfluid ^3He essentially isotropic¹. Consistent with this theoretical expectation, the experimental phase diagram of superfluid ^3He is indeed dominated by the isotropic B-phase.

A major surprise thus was the observation of the anisotropic, so-called A-phase of superfluid ^3He , occurring within the narrow window of low temperatures and high pressures¹. Its spin-ordered anisotropic nature arises from the spin-triplet p-wave Cooper pairing of the form ($l_z = 1, S_z = \pm 1$), containing only one of the three l_z values. In addition, the combination of the $S_z = \pm 1$ states (and the charge neutrality of ^3He) implies no net magnetization of the A-phase. The surprising and limited occurrence of the anisotropic A-phase of superfluid ^3He underlined its exotic nature.

Altermagnets represent the next physical realization of spin-ordered anisotropic zero-magnetization phases analogous to the A-phase of superfluid ^3He . In contrast to ^3He , however, the altermagnetic ordering was theoretically anticipated prior to the experimental discovery⁵. Moreover, the expectation was based not only on a microscopic theory applied to a specific physical system, but primarily on a general symmetry-based classification of crystal and spin structures⁴. As a result, hundreds of altermagnetic candidates have been identified, many of which order at ambient conditions, and not only in 3D inorganic materials^{4,5,18,19}, but also in 2D^{5,54–61} and organic crystals^{62,63}. The initial experimental demonstrations by momentum-space spectroscopic measurements have been performed in room-temperature altermagnetic materials MnTe and CrSb^{11,20–27}, representing simple binary compounds readily available in stable high-quality bulk or thin-film forms. The spectroscopy has been complemented in MnTe by direct-space vector-imaging and control of the altermagnetic ordering from micron-scale single-domain states to nano-scale domain walls and topological vortices⁶⁴.

Coming back to the anisotropic A-phase of ^3He , the intriguing question of its stability in the narrow region of temperatures and pressures was resolved by accounting for the additional complementary tendency of the ^3He fluid towards ferromagnetism. Under the right external conditions, this results in a spin-dependent effective interaction between the ^3He atoms, mediated by ferromagnetic fluctuations, which complements the long-range attractive van der Waals interaction and the short-range repulsion in the pairing mechanism⁶⁵.

The effective interactions and, in general, the vicinity of other (fluctuating) phases of the interacting Fermi fluid⁶⁶, has been a common theme considered across the field of the anisotropic phases, including the unconventional superconductors and nematic electronic

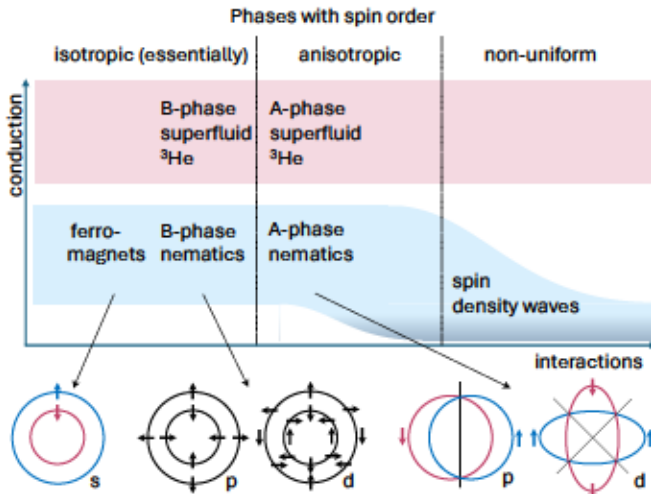


FIG. 3. Spin-ordered phases. Illustrative spin-ordered phases depicted in a conduction-type vs. interaction-strength diagram. Insets from left: Larger and smaller Fermi surfaces with opposite spin polarization of a model isotropic ferromagnet. Larger and smaller Fermi surfaces with opposite helicity of a model spin-ordered $l = 1$ (p-wave) nematic electronic liquid crystal in the B-phase, which is essentially isotropic. Corresponding spin-ordered $l = 2$ (d-wave) electronic nematic in the B-phase. Oppositely shifted spin-up and spin-down Fermi surfaces of a model spin-ordered $l = 1$ (p-wave) nematic in the A-phase, which is anisotropic. Corresponding spin-ordered $l = 2$ (d-wave) electronic nematic in the A-phase. (Recall that we use the term nematics in the generalized sense including all $l > 0$ even and odd-parity phases.)

liquid crystals without spin ordering, discussed in the previous section. Altermagnets stand apart also in this respect. Although intriguing physics may arise from an interplay of the altermagnetic phase with other order parameters of the interacting electrons^{5,7}, its stabilization relies, besides the exchange interaction, primarily on the external static single-particle potential of the underlying crystal lattice^{4,5,7,28}. The crystal potentials tend to be strong which adds to the robustness of altermagnets in conductive and insulating materials over a broad range of electron-electron interaction strengths.

This brings us to the last reference class of phases discussed in this Perspective. It is placed in the part of the diagram in Fig. 3 corresponding to metallic conduction and intermediate interaction strengths. The phases include conventional transition-metal ferromagnets and the theoretically considered spin-ordered electronic nematics. Together with the electronic nematics without spin ordering, mentioned in the previous section, their phenomenological description can be put under the common umbrella of Pomeranchuk Fermi liquid instabilities. We will now focus on the features of this theory that showed the direct link to the superfluid phases of ^3He , particularly to the A-phase,

and that allow us to explicitly demonstrate the analogous nature of ordering in altermagnets, as well as to further highlight what sets altermagnets apart.

Landau's theory of Fermi liquids considers two-body interactions between the quasiparticles. In a free space and for quasiparticles near the Fermi surface, the two-body interaction depends only on the angle θ between the linear momenta of the quasiparticles. Accordingly, it can be expanded in series of $\cos l\theta$ for 2D Fermi liquids, and of the l -th Legendre polynomials, $P_l(\cos \theta)$, for 3D Fermi liquids^{30,31}. Because of the correspondence to the orbital angular momentum wavefunctions, the index l is referred to as the l -th angular-momentum channel. In analogy to angular momentum, the $l = 0$ component corresponds to an isotropic interaction while the $l > 0$ components describe odd and even-parity anisotropic interaction. The prefactors of the expansion are the phenomenological Landau parameters, $F_l^{\text{c(s)}}$. Here the superscript c(s) labels the charge(spin) channel interaction given by the sum(difference) of interactions of the same-spin and opposite-spin quasiparticles.

Pomeranchuk derived a general form of the static susceptibility in each charge, spin and angular-momentum channel, finding it to be proportional to $1/(1+F_l^{\text{c(s)}})$. (Here $F_l^{\text{c(s)}}$ are conveniently normalized³¹.) The susceptibility diverges at $F_l^{\text{c(s)}} = -1$, signalling the Pomeranchuk instability of the Fermi liquid⁶⁷. The spin-channel $l = 0$ instability corresponds to a conventional isotropic (s-wave) ferromagnetic phase^{30,67}. The spin-degenerate Fermi surface of the normal state is split into larger and smaller Fermi surfaces, one corresponding to spin-up electrons and the other one to spin down electrons (Fig. 3). This breaks the rotation symmetry of the spin space. For the Fermi liquid in a free space, the split Fermi surfaces have an undistorted shape, respecting the continuous rotation symmetry of the free space. On a lattice, the ferromagnetic ground state preserves the discrete crystallographic point-group symmetries. (Recall that we are omitting the symmetry-breaking relativistic spin-orbit coupling terms present already in the Hamiltonian.)

The p-wave and d-wave nematic electronic liquid crystals without spin ordering, mentioned in the previous section and illustrated by the anisotropically distorted spin-degenerate Fermi surfaces in Fig. 2, correspond to the charge-channel Pomeranchuk instabilities in the $l = 1$ angular-momentum channel^{30,43–45,67} and $l = 2$ channel^{15,37,38}, respectively.

The spin-channel counterparts are illustrated in Fig. 3. Starting from the $l = 1$ (p-wave) channel, there are two types labeled as spin-ordered B-phase and A-phase electronic nematics¹⁷. In the former case, the Fermi surface spin-splits into larger and smaller surfaces, where the shape of each surface is otherwise undistorted^{13,14,68}. This is reminiscent of the $l = 0$ (s-wave) ferromagnetic phase, but there is a key difference. The spin-ordered B-phase electronic nematic has a momentum dependent

spin texture, where the direction of spin \mathbf{s} depends on the direction of momentum \mathbf{k} such that the spin winds once along the Fermi surface. As a result, the phase breaks, individually, both the spin-space and real-space rotation symmetries, while ferromagnets only break the spin-space symmetry. Nevertheless, the spin-ordered B-phase electronic nematic still remains essentially isotropic. This can be illustrated by defining a combined spin and real space helicity^{14,68}, $\mathbf{s} \cdot \mathbf{k}$, which is constant and has opposite sign on the two spin-split Fermi surfaces in the model of the spin-ordered $l = 1$ electronic nematic in the B-phase in Fig. 3. This is again reminiscent of the constant and opposite sign spin polarizations on the isotropic spin-split Fermi surfaces of the ferromagnet. However, while in the ferromagnet the opposite spin polarizations of the larger and smaller Fermi surface lead to a net magnetization, the helicity is an illustration of the zero net magnetization in the p-wave phase. Instead of the s-wave ferromagnet, the essentially isotropic spin-ordered electronic nematic in the B-phase is thus a direct counterpart of the superfluid ^3He in the B-phase¹⁴.

In contrast, the spin-channel $l = 1$ (p-wave) Pomeranchuk instability leading to the spin-ordered A-phase electronic nematic is an anisotropic phase^{12–14}. In Fig. 3, it is illustrated on spin-split Fermi surfaces shifted along one direction for one spin and the opposite direction for the opposite spin. Its spin-ordered anisotropic zero-magnetization nature makes it a direct counterpart of the superfluid ^3He in the A-phase¹⁴. The same correspondence between the A and B-phases of superfluid ^3He , on one hand, and the A and B-phases of spin-ordered electronic nematics, on the other hand, applies to the $l = 2$ (d-wave) channel¹⁷ (Fig. 3).

Fig. 4a shows a cartoon representation of spin-split Fermi surfaces of an altermagnet. The spin-ordered anisotropic zero-magnetization nature of the altermagnetic ordering is again a direct counterpart of the A-phase of superfluid ^3He . From the symmetry perspective of the distorted Fermi-surfaces, metallic altermagnets can be regarded as a realization of the spin-ordered electronic nematic in the A-phase. However, the physical mechanism that stabilizes the altermagnetic order in a broad range of materials, including also insulators, is principally distinct from the Pomeranchuk-instability mechanism stabilizing the nematic electronic liquid-crystal phases. In the latter case, the interactions have to be strong enough for the corresponding Landau parameter F_l^s to reach the critical value of the Pomeranchuk instability in the given l -channel while, simultaneously, the interactions have to be fine-tuned to avoid the instability in another l -channel. In particular, eliminating a pre-emptive/co-existing $l = 0$ ferromagnetic instability was recognized as one of the key challenges for realizing the spin-ordered $l > 0$ electronic nematics^{12,14,16,17}. Apart from the isotropic ferromagnetic ordering, a spin-density-wave phase can compete with the spin-ordered electronic nematic phase from the non-uniform side¹² of the diagram in Fig. 3. To

date, the spin-ordering nematic Fermi-liquid instabilities (without an interplay of strong spin-orbit coupling) have remained only as theoretical concepts.

In contrast, the altermagnetic ordering is stabilized in numerous materials by a combination of many-body electron-electron interactions and of comparably strong or even stronger effects of the single-particle potential of the ionic crystal lattice with a suitable symmetry^{4,5,7,28}. The electron-electron interactions lead to a collinear antiparallel ordering of spins and, upon an interplay with the crystal potential, the altermagnetic ordering acquires a characteristic symmetry $[C_2||A]$, where C_2 is a two-fold spin-space rotation and A is any real-space crystallographic rotation (proper or improper, symmorphic or non-symmorphic), and is not a real-space translation or inversion⁴. This symmetry protects zero net magnetization, i.e., excludes an s-wave ferromagnetic component. Simultaneously, it generates a characteristic $l > 0$ pattern of an alternating-sign spin density in the direct crystal space, and the corresponding $l > 0$ pattern of an alternating-sign spin-polarized electronic structure in the reciprocal momentum space⁷, as illustrated on the model d-wave altermagnet in Fig. 4a.

For comparison, in theories of the Pomeranchuk Fermi liquid instabilities, the crystal-lattice potential tends to enter only via a modification of the one-body momentum-dependent energy dispersion of the quasiparticle states. For example, Fermi-surface nesting effects in suitable lattice models were considered as a possible mechanism for favoring the anisotropic $l = 1$ spin-channel instability against the $l = 0$ ferromagnetic instability¹². Effects beyond quadratic dispersion of the quasiparticles were also shown to determine whether, for a critical value of a given Landau parameter $F_{l>0}^s$, the corresponding ordering will tend to be of the A-phase or the B-phase¹⁷.

The possibility of the formation of both the A-phase and the B-phase of the spin-ordered electronic nematics at the critical value of $F_{l>0}^s$ is another feature of these electronic liquid-crystal phases where altermagnets show a distinct phenomenology. The collinearity of the spin arrangement in altermagnets in both the direct crystal space and the reciprocal momentum space excludes the spin-textured type of ordering⁷. Altermagnets are thus counterparts of the A-phase of ^3He . (We again recall the omission of the symmetry-breaking spin-orbit coupling in the Hamiltonian.)

The collinearity also implies that the electronic structure has even parity, regardless of whether the magnetic crystal structure is centrosymmetric or non-centrosymmetric⁴. All 3D altermagnets can be classified⁴ by a systematic approach based on the spin-symmetry groups^{4,19,69–78} into d-wave ($l = 2$), g-wave ($l = 4$), or i-wave ($l = 6$) phases. The corresponding electronic structures are spin-degenerate at 2, 4, or 6 nodal surfaces in the Brillouin zone, respectively, and have alternating sign of the spin polarization outside these nodal surfaces⁴. The energy iso-surface of a given spin is distorted, breaking half of the crystallographic point-

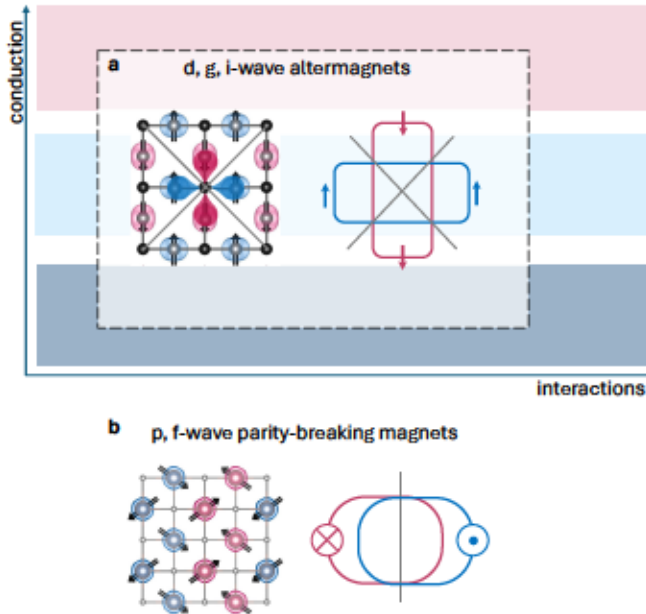


FIG. 4. Altermagnets and parity-breaking magnets. **a**, The correspondence between the altermagnetic ordering in the direct-space crystal structure and momentum-space electronic structure, occurring in materials over a broad range of interaction strengths and of different conduction types. The d-wave character of the direct-space spin density is highlighted around the central non-magnetic atom in the depicted model of a 2D altermagnet. The unpolarized nodes are highlighted by black lines. Corresponding d-wave electronic structure with equal-size split spin-up and spin-down energy iso-surfaces (Fermi surfaces), each breaking the four-fold rotation symmetry of the crystal lattice. The spin-degenerate nodes in the 2D Brillouin zone are again highlighted by black lines. **b**, The correspondence between the parity-breaking magnetic ordering in the direct-space crystal structure and momentum-space electronic structure. The collinear spin polarization of the split spin-up and spin-down energy iso-surfaces (Fermi surfaces) of the depicted model p-wave magnet are orthogonal to the plane of the non-collinear spins in the direct space.

group symmetries. The iso-surfaces corresponding to opposite spins are then mutually related by the second half of the crystallographic point-group symmetries.

We note that while theoretical realizations of nematic electronic liquid-crystal phases generated by the $l = 4$ and 6 spin-channel Pomeranchuk instabilities have not been considered in literature, numerous material candidates of not only d-wave, but also g-wave and i-wave altermagnets have been identified using the spin-group classification, supported by density-functional-theory calculations^{4,5,18,19}. The initial experimental spectroscopic confirmations were reported in g-wave altermagnets MnTe and CrSb^{11,20–27}.

Finally, we point out that a systematic theoretical exploration of the spin-ordered electronic nematics was largely motivated by spintronics¹⁴, a pattern that was repeated fifteen years later in altermagnets^{5,6,28}. Also

here, however, there is a significant difference. A detailed exploration of the spin-ordered $l = 1$ electronic nematic in the B-phase followed shortly after the theoretical predictions of the spin-Hall charge-to-spin conversion phenomenon in non-magnetic systems, generated by the relativistic spin-orbit coupling^{79,80}. The time-reversal invariant spin texture in the spin-ordered $l = 1$ electronic nematic in the B-phase was called a dynamically generated spin-orbit coupling because of the resemblance to the relativistic spin texture¹⁴. It was emphasized that compared to the perturbatively weak relativistic spin-orbit coupling, proportional to $1/c^2$ where c is the speed of light, the dynamically generated spin-orbit coupling could lead to significantly larger charge-to-spin conversion efficiency. However, an experimental realization of the spin-ordered B-phase (or A-phase) electronic nematics driven by the Pomeranchuk $l = 1$ spin-channel instability has remained elusive.

The search for the even-parity-wave altermagnets was motivated by a different spintronics incentive. It followed after several years of intense research of spintronics based on collinear antiferromagnets with spin-degenerate band structures⁸¹. The driving idea was to leverage the superior spatial, temporal and energy scalability demonstrated in antiferromagnetic spintronic devices, stemming from the compensated zero-magnetization ordering, while enabling strong spin-transport effects that underpin the technologically successful spintronics based on ferromagnets^{5,6,28}. As illustrated in Fig. 1, and reviewed in Refs. 5 and 6, the spin-polarized time-reversal symmetry breaking electronic structures generated by the compensated altermagnetic ordering enable this combination of merits, that were traditionally considered as mutually exclusive. Besides spintronics, the extraordinary nature of altermagnets is projected to be favorable in a range of research fields^{5–7}.

In summary, altermagnets share the spin-ordered anisotropic zero-magnetization nature with the A-phase of superfluid ^3He praised for its sophistication by Anthony Leggett in the Nobel lecture quote we used to open this article. In the case of altermagnets, however, the order is robust in many systems at room temperature and may end up being practically useful.

C. Beyond altermagnets towards parity-breaking p and f-wave magnets

In the previous section, we have left aside an apparent conflict between the theoretically considered nematic electronic liquid-crystal phases generated by the $l = 1$ Pomeranchuk instabilities, and the theorem by Bloch mentioned in Sec A, which states that the minimum energy state bears no current. The diverging susceptibilities at critical values of the Landau Fermi-liquid parameters, $F_l^{c(s)} = -1$, were identified by Pomeranchuk in all angular-momentum channels including $l = 1$. This seems to violate the above theorem.

When looking beyond the even-parity-wave altermagnets towards possible real physical realizations of the odd-parity p-wave magnetic phases, it is desirable to first revisit this apparent conflict. We will briefly do so before introducing the recently predicted abundance and robustness of the p-wave (as well as f-wave) magnetic ordering in real material candidates⁸².

The divergences of the charge and spin-channel susceptibilities for $l = 1$ order parameters were analyzed in Refs. 40–42. The studies started from the exact expression for the static susceptibility for a generic order parameter. It goes beyond the Pomeranchuk $\sim 1/(1 + F_l^{c(s)})$ form by including quasiparticle states away from the Fermi surface⁸³. For $l = 1$ order parameters corresponding to the current of conserved charge or spin, the divergencies in the generalized susceptibilities indeed disappear, regardless of the quasiparticle dispersion, i.e., both for the free-space Fermi liquid and in the presence of a crystal lattice^{40,41}. This is consistent with the above theorem by Bloch.

However, two possibilities were identified that could enable the phase transition from a Fermi liquid into a $l = 1$ electronic nematic liquid-crystal phase without or with spin ordering. One is a generic form of the order parameter which does not correspond to the charge or spin current⁴¹. The other one follows from the observation that even in the cases where the static susceptibility is non-diverging for the charge or spin-current order parameter, the instability of the Fermi-liquid ground state can still be signalled by the dynamic susceptibility⁴². The conclusion thus is that even within the framework of the Fermi-liquid instabilities, the parity-breaking p-wave magnetic phases are not formally excluded. Real physical realizations of such phases have, however, remained elusive.

This brings us to the very recent prediction of tens of material candidates of spin-ordered p-wave and f-wave zero-magnetization phases⁸². The prediction is based on an analogous classification of symmetries of spin arrangements on crystal lattices, supported by microscopic density-functional theory, that led to the identification of altermagnets. Since the spin-group symmetry analysis showed that odd-parity electronic structures were excluded for all collinear spin arrangements on crystals⁴, the search for the p-wave magnets, and odd-parity-wave magnets in general, turned to non-collinear spin arrangements. The identified favorable class has a non-collinear coplanar arrangement of spins in the direct crystal space, a symmetry $[C_2||t]$ combining a two-fold spin-space rotation along the common axis orthogonal to the spins and a real-space translation, and broken inversion symmetry. The $[C_2||t]$ symmetry protects zero net magnetization. Combined with the coplanarity, it also protects the single momentum-independent spin-polarization axis in the electronic structure which is orthogonal to the coplanar spins in the direct crystal space. Finally, the broken inversion symmetry allows for the splitting of the spin-up

and spin-down Fermi surfaces (or energy iso-surfaces in general).

A model example of the p-wave magnet satisfying the above symmetry conditions is shown in Fig. 4b. It represents yet another class of materials, besides altermagnets, which host the spin-ordered anisotropic zero-magnetization phase analogous to the A-phase of superfluid ^3He . The oppositely shifted distorted spin-up and spin-down Fermi surfaces in Fig. 4b can be viewed as a realization of the long-sought but elusive spin-ordered $l = 1$ electronic nematic in the A-phase^{12–14,17,40–42}. However, unlike the mechanism of Fermi-liquid instabilities, and like the mechanism stabilizing the altermagnetic ordering, the key feature of the identified candidate materials of the p-wave (as well as f-wave) magnetic ordering is the interplay in the direct space of electron-electron interactions and the single-particle potential of the crystal lattice with the suitable symmetries⁸².

We point out that space-groups of the identified p-wave and f-wave magnetic crystals break time-reversal symmetry but contain a symmetry combining time-reversal with translation. As a result, the point-groups of these parity-breaking magnets and, correspondingly, the energy spectra in the momentum space have time-reversal symmetry⁸². This contrasts with the even-parity-wave ordering in altermagnets which breaks time-reversal symmetry also in the point-group⁴. Finally, we note that the classification of symmetries of spin arrangements on crystal lattices, supported by density-functional theory calculations, has also led to the identification of material candidates with non-collinear magnetic structures whose electronic structure in the momentum space features a non-collinear spin-texture and can be regarded as a realization of the spin-ordered electronic nematics in the B-phase⁸⁴.

D. Summary

In this Perspective we have highlighted that the recently discovered altermagnets represent the next physical realization of the exotic type of ordering that was previously only observed in superfluid ^3He and theoretically envisaged in nematic electronic liquid crystals. The extraordinary nature of these phases is that they are spin-ordered and anisotropic, which is manifested in the spontaneous breaking of the spin-space and the real-space rotation symmetries and of the time-reversal symmetry, while having zero net magnetization. By going beyond these common basic signatures, we have reflected in more depth on microscopic physics of superfluid ^3He and the electronic liquid-crystal phases to shed light on what sets altermagnets apart. This can be summarized in the following points:

(i) The A-phase of superfluid ^3He was an experimental surprise. Prior microscopic calculations predicted the B-phase to be generally more stable. In contrast,

altermagnets were predicted by the systematic spin-symmetry group classification in a large family of materials which, together with microscopic density-functional-theory calculations, guided the initial experimental verifications.

(ii) The stability of the A-phase of superfluid ^3He in the narrow range of low temperatures and high pressures was ascribed to the interplay of internal interactions in the ^3He Fermi fluid, namely the short-range repulsion, the long-range attractive van der Waals interaction, and the effective interaction due to ferromagnetic fluctuations. Altermagnets are distinct in that the ordering is stabilized by the internal electron-electron (exchange) interaction, together with the robust external single-particle potential of the static crystal-lattice. In altermagnets the crystal structure is such that the antiparallel arrangement of spins necessarily implies anisotropy of spin-dependent properties.

(iii) The theories of nematic electronic liquid crystals focus on ordering in the momentum space, as arising from instabilities of the Fermi liquid. In contrast, altermagnets have the characteristic correspondence between the spin symmetries of the magnetic crystal-structure in the direct coordinate space, and of the spin-polarized electronic-structure in the reciprocal momentum space.

(iv) The formation of the spin-ordered electronic nematic phases was predicted to require a delicate balance of the interaction strength, exceeding the critical value for the $l > 0$ Fermi-liquid instability, while avoiding the conventional $l = 0$ ferromagnetic instability. In altermagnets, net magnetization is excluded (when omitting the spin-orbit coupling) by

the symmetry combining the spin-rotation and crystal-rotation transformations.

(v) The crystal potential, if considered, enters the theories of the spin-ordered electronic nematics indirectly via a modified one-body quasiparticle dispersion. In altermagnets, the external potential of the crystal lattice plays a direct central role. It is the glue which, together with the electron-electron interactions, holds the altermagnetic phase together.

As a result of these distinctive features, altermagnets are abundant and robust which, in combination with the extraordinary characteristics of the spin-ordered anisotropic zero-magnetization phases, suggests that they can open fruitful research directions in both science and technology.

Acknowledgments

TJ acknowledges support by the Ministry of Education of the Czech Republic CZ.02.01.01/00/22008/0004594 and, ERC Advanced Grant no. 101095925, RMF by the Air Force Office of Scientific Research under Award No. FA9550-21-1-0423, EF by the US National Science Foundation grant DMR 2225920 at the University of Illinois, AHM by the Robert A. Welch Foundation under Grant Welch F-2112 and by the Simons Foundation., and JS and LŠ acknowledge support by Deutsche Forschungsgemeinschaft (DFG, German Research Foundation) - DFG (Project 452301518) and TRR 288 – 422213477 (project A09).

¹ Leggett, A. J. Superfluid ^3He : The early days as seen by a theorist (2003). URL <https://www.nobelprize.org/uploads/2018/06/leggett-lecture.pdf>.

² Wölfele, P. Superfluid ^3He and unconventional superconductors. *Physica C: Superconductivity* **317–318**, 55–72 (1999). URL <https://linkinghub.elsevier.com/retrieve/pii/S0921453499000441>.

³ Tsuei, C. C. & Kirtley, J. R. Pairing symmetry in cuprate superconductors. *Reviews of Modern Physics* **72**, 969–1016 (2000).

⁴ Šmejkal, L., Sinova, J. & Jungwirth, T. Beyond Conventional Ferromagnetism and Antiferromagnetism: A Phase with Nonrelativistic Spin and Crystal Rotation Symmetry. *Physical Review X* **12**, 031042 (2022). URL <https://link.aps.org/doi/10.1103/PhysRevX.12.031042>. 2105.05820.

⁵ Šmejkal, L., Sinova, J. & Jungwirth, T. Emerging Research Landscape of Altermagnetism. *Physical Review X* **12**, 040501 (2022). URL <https://arxiv.org/abs/2204.10844>

⁶ Šmejkal, L., MacDonald, A. H., Sinova, J., Nakatsuji, S. & Jungwirth, T. Anomalous Hall antiferromagnets. *Nature Reviews Materials* **7**, 482–496 (2022). URL <https://arxiv.org/abs/2107.03321>

[//www.nature.com/articles/s41578-022-00430-3](https://www.nature.com/articles/s41578-022-00430-3). 2107.03321.

⁷ Jungwirth, T., Fernandes, R. M., Sinova, J. & Šmejkal, L. Altermagnets and beyond: Nodal magnetically-ordered phases 1–17 (2024). arXiv:2409.10034v1.

⁸ Lee, T. Y. *et al.* World-most energy-efficient MRAM technology for non-volatile RAM applications. In *2022 International Electron Devices Meeting (IEDM)*, 10.7.1–10.7.4 (IEEE, 2022). URL <https://ieeexplore.ieee.org/document/10019430/>.

⁹ Ambrosi, E. *et al.* Low voltage (1.8 V) and high endurance (1M) 1-Selector/1-STT-MRAM with ultra-low (1 ppb) read disturb for high density embedded memory arrays. In *2023 International Electron Devices Meeting (IEDM)*, 1–4 (IEEE, 2023). URL <https://ieeexplore.ieee.org/document/10413809/>.

¹⁰ IRDS 2023 update: Beyond CMOS and Emerging Materials Integration. Tech. Rep. (2023). URL https://irds.ieee.org/images/files/pdf/2023/2023IRDS_BC.pdf.

¹¹ Krempaský, J. *et al.* Altermagnetic lifting of Kramers spin degeneracy. *Nature* **626**, 517–522 (2024). URL <https://doi.org/10.1038/s41586-023-06907-7> <https://www.nature.com/articles/s41586-023-06907-7> <https://arxiv.org/abs/2308.10681>. 2308.10681.

¹² Hirsch, J. E. Spin-split states in metals. *Physical Review B* **41**, 6820–6827 (1990). URL <https://journals.aps.org/prb/abstract/10.1103/PhysRevB.41.6820> <https://link.aps.org/doi/10.1103/PhysRevB.41.6820>.

¹³ Marchenko, V. I. Theory of spin ordering in metals. *JETP Lett.* **54**, 514 (1991).

¹⁴ Wu, C. & Zhang, S. C. Dynamic generation of spin-orbit coupling. *Physical Review Letters* **93** (2004).

¹⁵ Fradkin, E., Kivelson, S. A. & Oganesyan, V. Electron Nematic Phase in a Transition Metal Oxide. *Science* **315**, 196–197 (2007). URL <https://www.science.org/doi/10.1126/science.1137172>.

¹⁶ Fischer, M. H. & Kim, E.-A. Mean-field analysis of intra-unit-cell order in the Emery model of the CuO₂ plane. *Physical Review B* **84**, 144502 (2011). URL <https://link.aps.org/doi/10.1103/PhysRevB.84.144502>.

¹⁷ Wu, C., Sun, K., Fradkin, E. & Zhang, S.-C. Fermi liquid instabilities in the spin channel. *Physical Review B* **75**, 115103 (2007). URL <https://journals.aps.org/prb/pdf/10.1103/PhysRevB.75.115103> <https://link.aps.org/doi/10.1103/PhysRevB.75.115103>.

¹⁸ Guo, Y. *et al.* Spin-split collinear antiferromagnets: A large-scale ab-initio study. *Materials Today Physics* **32**, 100991 (2023). URL <https://linkinghub.elsevier.com/retrieve/pii/S2542529323000275> [2207.07592](https://doi.org/10.1016/j.mtphys.2023.100991).

¹⁹ Xiao, Z., Zhao, J., Li, Y., Shindou, R. & Song, Z.-D. Spin Space Groups: Full Classification and Applications. *Arxiv Preprint* 1–1664 (2023). URL <http://arxiv.org/abs/2307.10364> [2307.10364](https://doi.org/10.4236/jmp.2023.133001).

²⁰ Lee, S. *et al.* Broken Kramers Degeneracy in Altermagnetic MnTe. *Physical Review Letters* **132**, 036702 (2024). URL <http://arxiv.org/abs/2308.11180> <https://link.aps.org/doi/10.1103/PhysRevLett.132.036702> [2308.11180](https://doi.org/10.1103/PhysRevLett.132.036702).

²¹ Osumi, T. *et al.* Observation of a giant band splitting in altermagnetic MnTe. *Physical Review B* **109**, 115102 (2024). URL <https://link.aps.org/doi/10.1103/PhysRevB.109.115102>.

²² Hajlaoui, M. *et al.* Temperature Dependence of Relativistic Valence Band Splitting Induced by an Altermagnetic Phase Transition. *Advanced Materials* (2024). URL <https://onlinelibrary.wiley.com/doi/10.1002/adma.202314076>.

²³ Reimers, S. *et al.* Direct observation of altermagnetic band splitting in CrSb thin films. *Nature Communications* **15**, 2116 (2024). URL <https://www.nature.com/articles/s41467-024-46476-5> [2310.17280](https://doi.org/10.1038/s41467-024-46476-5).

²⁴ Yang, G. *et al.* Three-dimensional mapping and electronic origin of large altermagnetic splitting near Fermi level in CrSb (2024). URL <http://arxiv.org/abs/2405.12575> [2405.12575](https://doi.org/10.4236/jmp.20240512575).

²⁵ Ding, J. *et al.* Large band-splitting in *g*-wave type altermagnet CrSb (2024). URL <http://arxiv.org/abs/2405.12687> [2405.12687](https://doi.org/10.4236/jmp.20240512687).

²⁶ Li, C. *et al.* Topological Weyl Altermagnetism in CrSb (2024). URL <https://arxiv.org/abs/2405.14777> [2405.14777](https://doi.org/10.4236/jmp.20240514777).

²⁷ Lu, W. *et al.* Observation of surface Fermi arcs in altermagnetic Weyl semimetal CrSb (2024). URL <https://arxiv.org/abs/2407.13497> [2407.13497](https://doi.org/10.4236/jmp.20240713497).

²⁸ Šmejkal, L., González-Hernández, R., Jungwirth, T. & Sinova, J. Crystal time-reversal symmetry breaking and spontaneous Hall effect in collinear antiferromagnets. *Science Advances* **6**, eaaz8809 (2020). URL <https://www.science.org/doi/10.1126/sciadv.aaz8809> [1901.00445](https://doi.org/10.1126/sciadv.aaz8809).

²⁹ Bai, L. *et al.* Altermagnetism: Exploring New Frontiers in Magnetism and Spintronics. *Arxiv Preprint* 1–49 (2024). URL <https://arxiv.org/pdf/2406.02123.pdf> [2406.02123](https://arxiv.org/abs/2406.02123).

³⁰ Landau, L. D. The Theory of a Fermi Liquid. *Sov. Phys. JETP* **3**, 920 (1957).

³¹ Vignale, G. Fermi Liquids. In Pavarini, E., Koch, E., Lichtenstein, A. & Vollhardt, D. (eds.) *Dynamical mean-field theory of correlated electrons* (2022).

³² Bardeen, J., Cooper, L. N. & Schrieffer, J. R. Theory of Superconductivity. *Physical Review* **108**, 1175–1204 (1957). URL <https://link.aps.org/doi/10.1103/PhysRev.108.1175>.

³³ Kivelson, S. A., Fradkin, E. & Emery, V. J. Electronic liquid-crystal phases of a doped Mott insulator. *Nature* **393**, 550–553 (1998). URL <https://www.nature.com/articles/31177>.

³⁴ Fradkin, E. & Kivelson, S. A. Liquid-crystal phases of quantum Hall systems. *Physical Review B* **59**, 8065–8072 (1999). URL <https://link.aps.org/doi/10.1103/PhysRevB.59.8065>.

³⁵ Rezayi, E. H., Haldane, F. D. M. & Yang, K. Charge-Density-Wave Ordering in Half-Filled High Landau Levels. *Physical Review Letters* **83**, 1219–1222 (1999). URL <https://link.aps.org/doi/10.1103/PhysRevLett.83.1219>.

³⁶ Jungwirth, T., MacDonald, A. H., Smrčka, L. & Girvin, S. M. Field-tilt anisotropy energy in quantum Hall stripe states. *Physical Review B* **60**, 15574–15577 (1999). URL <https://link.aps.org/doi/10.1103/PhysRevB.60.15574>.

³⁷ Halboth, C. J. & Metzner, W. d-Wave Superconductivity and Pomeranchuk Instability in the Two-Dimensional Hubbard Model. *Physical Review Letters* **85**, 5162–5165 (2000). URL <https://link.aps.org/doi/10.1103/PhysRevLett.85.5162>.

³⁸ Oganesyan, V., Kivelson, S. A. & Fradkin, E. Quantum theory of a nematic Fermi fluid. *Physical Review B* **64**, 195109 (2001). URL <https://link.aps.org/doi/10.1103/PhysRevB.64.195109>.

³⁹ Kivelson, S. A. *et al.* How to detect fluctuating stripes in the high-temperature superconductors. *Reviews of Modern Physics* **75**, 1201–1241 (2003). [0210683](https://doi.org/10.1103/PhysRevLett.83.1219).

⁴⁰ Kiselev, E. I., Scheurer, M. S., Wölfle, P. & Schmalian, J. Limits on dynamically generated spin-orbit coupling: Absence of 1=1 Pomeranchuk instabilities in metals. *Physical Review B* **95**, 125122 (2017). URL <https://journals.aps.org/prb/abstract/10.1103/PhysRevB.95.125122> <https://link.aps.org/doi/10.1103/PhysRevB.95.125122> [1611.01442](https://doi.org/10.1103/PhysRevB.95.125122).

⁴¹ Wu, Y.-M., Klein, A. & Chubukov, A. V. Conditions for 1=1 Pomeranchuk instability in a Fermi liquid. *Physical Review B* **97**, 165101 (2018). URL <https://journals.aps.org/prb/abstract/10.1103/PhysRevB.97.165101> [http://arxiv.org/abs/1801.06571](https://arxiv.org/abs/1801.06571) <https://doi.org/10.1103/PhysRevB.97.165101> <https://link.aps.org/doi/10.1103/PhysRevB.97.165101> [1801.06571](https://doi.org/10.1103/PhysRevB.97.165101).

⁴² Klein, A., Maslov, D. L., Pitaevskii, L. P. & Chubukov, A. V. Collective modes near a Pomeranchuk instability in two dimensions. *Physical Review Research* **1**, 033134 (2019). URL <https://link.aps.org/doi/10.1103/PhysRevResearch.1.033134> [1901.00445](https://doi.org/10.1103/PhysRevResearch.1.033134).

1103/PhysRevResearch.1.033134.

⁴³ Born, M. & Cheng, K. C. Theory of Superconductivity. *Nature* **161**, 968–969 (1948). URL <https://www.nature.com/articles/161968a0>.

⁴⁴ Bohm, D. Note on a Theorem of Bloch Concerning Possible Causes of Superconductivity. *Physical Review* **75**, 502–504 (1949). URL <https://link.aps.org/doi/10.1103/PhysRev.75.502>.

⁴⁵ Hoddeson, L., Baym, G. & Eckert, M. The development of the quantum-mechanical electron theory of metals: 1928–1933. *Reviews of Modern Physics* **59**, 287–327 (1987). URL <https://link.aps.org/doi/10.1103/RevModPhys.59.287>.

⁴⁶ Schmalian, J. Failed theories of superconductivity. *Modern Physics Letters B* **24**, 2679–2691 (2010). URL <https://www.worldscientific.com/doi/abs/10.1142/S0217984910025280>.

⁴⁷ Lilly, M. P., Cooper, K. B., Eisenstein, J. P., Pfeiffer, L. N. & West, K. W. Evidence for an Anisotropic State of Two-Dimensional Electrons in High Landau Levels. *Physical Review Letters* **82**, 394–397 (1999). URL <https://link.aps.org/doi/10.1103/PhysRevLett.82.394>.

⁴⁸ Borzi, R. A. *et al.* Formation of a Nematic Fluid at High Fields in Sr₃Ru₂O₇. *Science* **315**, 214–218 (2007). URL <https://www.science.org/doi/10.1126/science.1134796>.

⁴⁹ Fradkin, E., Kivelson, S. A., Lawler, M. J., Eisenstein, J. P. & Mackenzie, A. P. Nematic fermi fluids in condensed matter physics. *Annual Review of Condensed Matter Physics* **1**, 153–178 (2010). 0910.4166.

⁵⁰ Fernandes, R. M., Chubukov, A. V. & Schmalian, J. What drives nematic order in iron-based superconductors? *Nature Physics* **10**, 97–104 (2014).

⁵¹ Lee, K., Shao, J., Kim, E.-A., Haldane, F. D. M. & Rezayi, E. H. Pomeranchuk Instability of Composite Fermi Liquids. *Physical Review Letters* **121**, 147601 (2018). URL <https://doi.org/10.1103/PhysRevLett.121.147601> <https://link.aps.org/doi/10.1103/PhysRevLett.121.147601.1802.08261>.

⁵² Quintanilla, J. & Ciftja, O. Asymptotic Pomeranchuk instability of Fermi liquids in half-filled Landau levels. *Scientific Reports* **13**, 1400 (2023). URL <https://doi.org/10.1038/s41598-023-28614-z> <https://www.nature.com/articles/s41598-023-28614-z>.

⁵³ Andreev, A. & Grishchuk, I. Spin nematics. *Sov. Phys. JETP* **60**, 267 (1984).

⁵⁴ Šmejkal, L., Hellenes, A. B., González-Hernández, R., Sinova, J. & Jungwirth, T. Giant and Tunneling Magnetoresistance in Unconventional Collinear Antiferromagnets with Nonrelativistic Spin-Momentum Coupling. *Physical Review X* **12**, 011028 (2022). URL <https://link.aps.org/doi/10.1103/PhysRevX.12.011028> <https://arxiv.org/abs/2103.12664>. 2103.12664.

⁵⁵ Ma, H.-Y. *et al.* Multifunctional antiferromagnetic materials with giant piezomagnetism and noncollinear spin current. *Nature Communications* **12**, 2846 (2021). URL <https://doi.org/10.1038/s41467-021-23127-7> <https://www.nature.com/articles/s41467-021-23127-7>. arXiv:2104.00561.

⁵⁶ Egorov, S. A. & Evarestov, R. A. Colossal Spin Splitting in the Monolayer of the Collinear Antiferromagnet MnF₂. *The Journal of Physical Chemistry Letters* **12**, 2363–2369 (2021). URL <https://pubs.acs.org/doi/10.1021/acs.jpclett.1c00282>.

⁵⁷ Brekke, B., Brataas, A. & Sudbø, A. Two-dimensional altermagnets: Superconductivity in a minimal microscopic model. *Physical Review B* **108**, 224421 (2023). URL <http://arxiv.org/abs/2308.08606> <https://link.aps.org/doi/10.1103/PhysRevB.108.224421>. 2308.08606.

⁵⁸ Cui, Q., Zhu, Y., Yao, X., Cui, P. & Yang, H. Giant spin-Hall and tunneling magnetoresistance effects based on a two-dimensional nonrelativistic antiferromagnetic metal. *Physical Review B* **108**, 024410 (2023). URL <https://journals.aps.org/prb/abstract/10.1103/PhysRevB.108.024410> <https://link.aps.org/doi/10.1103/PhysRevB.108.024410>.

⁵⁹ Chen, X., Wang, D., Li, L. & Sanyal, B. Giant spin-splitting and tunable spin-momentum locked transport in room temperature collinear antiferromagnetic semimetallic CrO monolayer. *Applied Physics Letters* **123** (2023). URL <https://pubs.aip.org/apl/article/123/2/022402/2901960/Giant-spin-splitting-and-tunable-spin-momentum>.

⁶⁰ Mazin, I., González-Hernández, R. & Šmejkal, L. Induced Monolayer Altermagnetism in MnP(S,Se)₃ and FeSe. *2*, 1–11 (2023). URL <http://arxiv.org/abs/2309.02355>. 2309.02355.

⁶¹ Södequist, J. & Olsen, T. Two-dimensional altermagnets from high throughput computational screening: symmetry requirements, chiral magnons and spin-orbit effects 1–7 (2024). URL <http://arxiv.org/abs/2401.05992>. 2401.05992.

⁶² Naka, M. *et al.* Spin current generation in organic antiferromagnets. *Nature Communications* **10**, 4305 (2019). URL <http://dx.doi.org/10.1038/s41467-019-12229-y> <http://www.nature.com/articles/s41467-019-12229-y> <https://doi.org/10.1038/s41467-019-12229-y>. 1902.02506.

⁶³ Ferrari, F. & Valenti, R. Altermagnetism on the Shastry-Sutherland lattice (2024). URL <http://arxiv.org/abs/2408.00841>. 2408.00841.

⁶⁴ Amin, O. J. *et al.* Nanoscale imaging and control of altermagnetism in MnTe. *Nature* *in press*. URL <https://arxiv.org/abs/2405.02409> <http://arxiv.org/abs/2405.02409>. 2405.02409.

⁶⁵ Anderson, P. W. & Brinkman, W. F. Anisotropic Superfluidity in He₃ : A Possible Interpretation of It. *Physical Review Letters* **30**, 1108–1111 (1973). URL <https://link.aps.org/doi/10.1103/PhysRevLett.30.1108>.

⁶⁶ Schofield, A. J., Conduit, G. J., Green, A. G. & Simons, B. D. Viewpoint There and back again: from magnets to superconductors Subject Areas: Magnetism, Superconductivity A Viewpoint on: Inhomogeneous Phase Formation on the Border of Itinerant Ferromagnetism. *Phys. Rev. Lett* **2**, 207201 (2009). URL <https://physics.aps.org/articles/pdf/10.1103/Physics.2.93.0908.4433>.

⁶⁷ Pomeranchuk, I. On the stability of a Fermi liquid. *Phys. JETP* **8**, 361–362 (1959).

⁶⁸ Akhiezer, I. & Chudnovskii, E. Polarized electrons from non-ferromagnetic metals? *Physics Letters A* **65**, 433–434 (1978). URL <https://linkinghub.elsevier.com/retrieve/pii/0375960178904620>.

⁶⁹ Litvin, D. B. & Opechowski, W. Spin groups. *Physica* **76**, 538–554 (1974). URL <https://linkinghub>.

elsevier.com/retrieve/pii/0031891474901578 <https://www.sciencedirect.com/science/article/abs/pii/0031891474901578?via%3Dihub>.

⁷⁰ Litvin, D. B. Spin point groups. *Acta Crystallographica Section A* **33**, 279–287 (1977). URL <http://scripts.iucr.org/cgi-bin/paper?S0567739477000709>

⁷¹ Liu, P., Li, J., Han, J., Wan, X. & Liu, Q. Spin-Group Symmetry in Magnetic Materials with Negligible Spin-Orbit Coupling. *Physical Review X* **12**, 21016 (2022). URL <http://arxiv.org/abs/2103.15723> <https://link.aps.org/doi/10.1103/PhysRevX.12.021016>. 2103.15723.

⁷² McClarty, P. A. & Rau, J. G. Landau Theory of Altermagnetism. *Physical Review Letters* **132**, 176702 (2024). URL <https://link.aps.org/doi/10.1103/PhysRevLett.132.176702>.

⁷³ Smolyanyuk, A., Šmejkal, L. & Mazin, I. I. A tool to check whether a symmetry-compensated collinear magnetic material is antiferro- or altermagnetic 1–16 (2024). URL <http://arxiv.org/abs/2401.08784>. 2401.08784.

⁷⁴ Shinohara, K. *et al.* Algorithm for spin symmetry operation search. *Acta Crystallographica Section A Foundations and Advances* **80**, 94–103 (2024). URL <https://scripts.iucr.org/cgi-bin/paper?S2053273323009257>.

⁷⁵ Watanabe, H., Shinohara, K., Nomoto, T., Togo, A. & Arita, R. Symmetry analysis with spin crystallographic groups: Disentangling effects free of spin-orbit coupling in emergent electromagnetism. *Physical Review B* **109**, 094438 (2024). URL <https://link.aps.org/doi/10.1103/PhysRevB.109.094438>.

⁷⁶ Jiang, Y. *et al.* Enumeration of spin-space groups: Towards a complete description of symmetries of magnetic orders (2023). URL <http://arxiv.org/abs/2307.10371>. 2307.10371.

⁷⁷ Ren, J. *et al.* Enumeration and representation of spin space groups. *Arxiv Preprint* (2023). URL <http://arxiv.org/abs/2307.10369>. 2307.10369.

⁷⁸ Schiff, H., Corticelli, A., Guerreiro, A., Romhányi, J. & McClarty, P. The Spin Point Groups and their Representations (2023). URL <http://arxiv.org/abs/2307.12784>. 2307.12784.

⁷⁹ Murakami, S., Nagaosa, N. & Zhang, S.-C. Dissipationless Quantum Spin Current at Room Temperature. *Science (New York, N.Y.)* **301**, 1348–1351 (2003).

⁸⁰ Sinova, J. *et al.* Universal intrinsic spin Hall effect. *Physical Review Letters* **92**, 126603 (2004). 0307663.

⁸¹ Jungwirth, T. *et al.* The multiple directions of antiferromagnetic spintronics. *Nature Physics* **14**, 200–203 (2018). URL <http://www.nature.com/articles/s41567-018-0063-6>.

⁸² Hellenes, A. B. *et al.* P-wave magnets. *Arxiv Preprint* (2023). URL <http://arxiv.org/abs/2309.01607>. 2309.01607.

⁸³ Leggett, A. J. Theory of a Superfluid Fermi Liquid. I. General Formalism and Static Properties. *Physical Review* **140**, A1869–A1888 (1965). URL <https://link.aps.org/doi/10.1103/PhysRev.140.A1869>.

⁸⁴ Hellenes, A. B., Jungwirth, T., Sinova, J. & Šmejkal, L. Exchange spin-orbit coupling and unconventional p-wave magnetism (2023). URL <http://arxiv.org/abs/2309.01607v1>. 2309.01607v1.